Analysis of THz generation by multicolor laser pulses with various frequency ratios

Zhaoyan Zhou,[1,*] Zhihui lv,[1] Dongwen Zhang,[1] Zengxiu Zhao,[1] and C. D. Lin[2]

[1]*Department of Physics, College of Science, National University of Defense Technology, Changsha 410073, People's Republic of China*
[2]*Department of Physics, Cardwell Hall, Kansas State University, Manhattan, Kansas 66506, USA*

Terahertz (THz) generation in a gas medium is simulated by quantum calculations with multicolor intense laser pulses of various frequency ratios. By correlating THz radiation with the above-threshold-ionization photoelectron spectrum, we confirm that our previously proposed free-free transition model for the generation of THz radiation is also applicable to multicolor pulses. THz photon emissions can proceed through transitions between continuous states with similar energies that have opposite parities. This mechanism predicts that THz waves can be efficiently generated at special two-color laser frequency ratios when the multiphoton mixing condition is satisfied. Applying this model to multicolor fields (sawtooth wave shape), we provide a quantum-mechanical interpretation for the reason for THz radiation enhancement. A scheme combining multiple lasers to raise THz radiation satisfying multiphoton mixing conditions is also proposed.

I. INTRODUCTION

Terahertz (THz) radiation has gained wide attention in recent years because of its multitude of applications in physics, medical imaging, and security [1,2]. Generation of intense THz sources remains a major challenge for these applications. Among various experimental schemes, it is widely accepted that an effective THz generation is to focus intense laser pulses into a gas cell to create a plasma. THz waves are emitted by the ionized electrons from individual gas target atoms or molecules in the low-pressure limit [3–6]. Many theoretical calculations have been carried out in the last few decades by solving the time-dependent Schrödinger equation (TDSE) [7–11] to study THz signals in an effort to find efficient methods that would benefit THz generation.

Up to now, it has been widely accepted that THz can be efficiently generated by using a two-color pulse, and the laser frequency has mostly been taken with the ratio $\omega_2 : \omega_1 = 2 : 1$ [12–16]. Here ω_1 and ω_2 are usually the frequencies of the 800- and 400-nm lasers, respectively. Since 2013, it has also been proposed that other frequency combinations could also enhance THz emission [17,18]. In 2016, Kostin *et al.* [19] showed that THz emission can be enhanced when the frequency ratio corresponds to a rational fraction. Experimentally, Zhang *et al.* [20] demonstrated efficient THz generation for two-color laser fields with special frequency ratios, such as $400 + 1600$ and $800 + 1200$ nm. In addition, González de Alaiza Martínez *et al.* [21] proposed that a multicolor laser pulse with a sawtooth wave shape could also significantly increase the THz radiation. With these new combinations of laser pulses, the mechanism for THz emission is often explained with the semiclassical photocurrent (PC) model [17,18,20,21] or the nonlinear multiwave mixing model [19].

The above models have achieved great success in explaining the THz radiation mechanism and providing good guidance for experiments. However, most of them are based on semiclassical theory. It will be a useful supplement to discuss the THz radiation mechanism from the perspective of THz photon radiation. In 2017, we calculated the THz radiation as well as the above-threshold-ionization (ATI) photoelectron spectrum simultaneously by solving the quantum-mechanical TDSE for a $(800 + 400)$-nm two-color laser field [22]. We were able to correlate THz emission with the asymmetry of the ATI photoelectrons along the "left" versus the "right" side of the linear polarization axis of the laser. In addition, we showed that the degree of overlap between even-parity-dominant electrons and odd-parity-dominant electrons within each ATI peak directly determines the strength of THz emission. This conclusion helps to explain THz generation based on the quantum picture. It also favors the model that THz is generated through free-free transitions of electron wave packets associated with ATI peaks.

In this paper, we extend this method and calculate THz generation and ATI spectrum simultaneously in laser fields with uncommon frequency ratios, including the two- and multicolor cases, by solving the TDSE. We verified the same correlation between THz generation and ATI spectra for various laser frequency combinations. By associating THz radiation with the occupancy distribution of the continuous electron states, we identified the mechanism of THz radiation from the multiphoton ionization pathways to reach continuum states of semiequal energies of opposite parities. Free-free transitions between such states are attributed as the main mechanism of THz generation. Based on such analysis, conditions for advantageous generation of THz radiation in multifrequency combined laser fields are theoretically verified.

In the remainder of the paper, we first summarize how the calculations were carried out. Then the main results are presented together with a discussion of the theoretical model for interpreting the calculated results, including THz generation

*cnzhzhy@nudt.edu.cn

by two- and multicolor laser pulses with various frequency ratios. The last section concludes the findings of this work.

II. THEORETICAL METHODS

We calculate the THz spectrum and the photoelectron momentum spectra by numerical solution of the three-dimensional (3D) TDSE,

$$i\frac{\partial}{\partial t}\psi(\mathbf{r},t) = (\hat{H}_0 + \hat{H}_I)\psi(\mathbf{r},t), \quad (1)$$

where $\hat{H}_0$ is the field-free Hamiltonian and $\hat{H}_I$ is the interaction term of the atom with the laser field, given in the length gauge. Atomic units (a.u.) are used unless otherwise indicated.

In the dipole approximation,

$$\hat{H}_I = -\mathbf{E}(\mathbf{t}) \cdot \mathbf{r}, \quad (2)$$

where $\mathbf{E}(\mathbf{t})$ is the incident laser field. The laser is linearly polarized; thus, we have to consider only the $m = 0$ component of the magnetic quantum number of the atom. The time-dependent wave function $\psi(\mathbf{r},t)$ is expanded with Legendre polynomials in the θ coordinate as

$$\psi(r_i, x_j, t) = \sum_{l=0}^{L} c_l(t) R_l(r_i) P_l(x_j), \quad x_j = \cos\theta_j, \quad (3)$$

and the radial function $R_l(r)$ is expanded using the discrete-variable-representation (DVR) basis set associated with Legendre polynomials [23–25]. The coefficients c_l can be calculated using the split-operator method [26]. Here we expand the wave functions with 4000 DVR points for $r_{max} = 2000$ a.u. and 120 partial waves. Once the time-dependent wave function is determined, the induced dipole moment is calculated using the acceleration form

$$a(t) = \langle\psi(\mathbf{r},t)|\frac{\partial V}{\partial z}|\psi(\mathbf{r},t)\rangle, \quad (4)$$

where V is the total potential field that the electron experiences, including Coulomb and laser-electron interaction potentials. The emission spectrum including the THz emission can be obtained by Fourier transformation of the time-dependent dipole moment [9]. To obtain the THz spectrum without continuing the calculation to the long time of several picoseconds, in fact, we use the wavelet analysis to sample the frequency of the radiation in the THz region. This is performed by a wavelet transformation [27]:

$$A_\omega(t_0, \omega) = \int a(t) w_{t_0,\omega}(t) dt, \quad (5)$$

with the wavelet kernel $w_{t_0,\omega}(t) = \sqrt{\omega}W[\omega(t - t_0)]$, where $W[x] = \frac{1}{\sqrt{\tau}}e^{ix}e^{-x^2/2\tau^2}$. τ is chosen to be 5 a.u., and ω is 18 THz (0.0028 a.u.), which is the peak frequency of the THz wave according to our previous study [10]. If τ is increased to 15 a.u., the spectrum would not change much. Changing the duration and the wavelength of the laser fields will have an effect on the THz wave form [9,28–30], while the time profile calculated from Eq. (5) does not change much. In other words, $A_\omega(t_0, \omega)$ is insensitive to changes in ω within a few terahertz.

The two- or multicolor laser fields used here will result in an asymmetric photoelectron spectrum. The two-dimensional

electron momentum distribution can be calculated by projecting out the final time-dependent wave function at the end of the laser pulse to the eigenstates of the continuum electron of momentum $\mathbf{p}$ [27]:

$$\frac{\partial^2 P}{\partial E \partial\theta} = |\langle\Phi_p^-|\psi(t = t_f)\rangle|^2 2\pi p \sin\theta, \quad (6)$$

where $E = p^2/2$ is the kinetic energy of the photoelectron and θ is the angle between the momentum vector $\mathbf{p}$ and the laser polarization directions (along the z axis). The electron energy spectrum can be obtained by integrating over θ,

$$\frac{\partial P}{\partial E} = \int \frac{\partial^2 P}{\partial E \partial\theta} d\theta. \quad (7)$$

The asymmetry of the ATI spectrum is defined by [31,32]

$$A = (P_+ - P_-)/(P_+ + P_-), \quad (8)$$

where $P_\pm$ is the electron spectrum strength on the $\pm z$ sides from Eq. (7) by setting the integration range to be 0 to $\pi/2$ and from $\pi/2$ to π, respectively.

III. ANALYSIS OF THz GENERATION IN TWO-COLOR LASER FIELDS OF VARIOUS FREQUENCY RATIOS

A. Asymmetry of the average electron velocity vs THz generation

We first make calculations for a hydrogen atom in two-color laser fields,

$$E(t) = E_L f(t)[\cos(\omega_1 t) + \cos(\omega_2 t + \varphi)], \quad (9)$$

where E_L is the amplitude of the incident laser field. We fix the wavelength of the first laser at 800 nm and change the wavelength of the second laser so that the frequencies of the two incident laser pulses satisfy a certain ratio. The same envelope of the laser pulse, $f(t)$, is chosen for both laser frequencies. It takes the sine-square form, and the duration is 20 optical cycles (oc) of the 800-nm laser field.

Because THz strength can be strongly affected by the ionization probability, we adjusted the laser amplitude E_L as ω_2 is varied to maintain the maximum free-electron density at the 1% level. The free-electron density can be calculated using the Ammosov-Delone-Krainov model [27].

THz has been widely interpreted using the PC model [11,33]. In the quantum calculations performed here, we have used Eq. (4) to calculate the acceleration. We define an average velocity from the dipole acceleration of Eq. (4) via

$$v(t) = \int_{-\infty}^{t} a(t') dt'. \quad (10)$$

From a classical point of view, the electron current can be related to its average velocity. It has been pointed out that THz emissions are enhanced when the frequency ratios of the two-color laser fields take some special values [19,20], such as $\omega_2 : \omega_1 = 1 : 4, 2 : 3$, and $3 : 2$. Figure 1(a) shows the average velocity calculated according to Eq. (10). It can be seen in Fig. 1(a) that in addition to the oscillatory feature, a nonzero DC electron current appears along with the laser pulse. According to the PC model, the THz wave is in proportion to the transient current of ionized electrons. It is expected that the
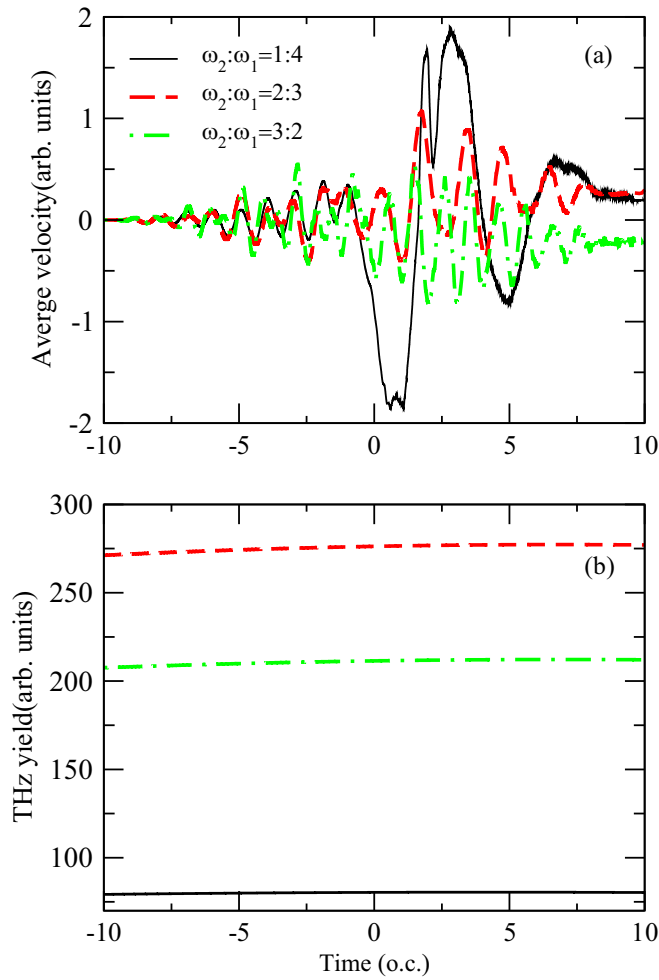
FIG. 1. (a) The average time-varying electron velocities for a hydrogen atom in two-color laser fields for frequency ratios $\omega_2 : \omega_1 = 1 : 4$ (black), $2 : 3$ (red), and $3 : 2$ (green). (b) The corresponding time profile of the 18-THz radiation. The first pulse (ω_1) is fixed to be an 800-nm, 20-oc, and sine-square enveloped infrared laser pulse. The relative phases φ were set to 0, 0, and 0.5π for the three cases to guarantee that THz radiation is near the maximum. The laser intensities are chosen such that the ionization level is fixed at 1% after the pulse is over. The intensities are 3.54, 3.48, and 3.48 in units of 10^{13} W/cm^2, respectively.

intensity of THz radiation can be qualitatively related to the average velocity of the electron. From the oscillatory feature, it appears that asymmetry is largest for $\omega_2 : \omega_1 = 2 : 3$, then $3 : 2$, and smallest for $1 : 4$. We calculate the integral of each curve in Fig. 1(a); their respective DC terms are 2.65, -2.10, and 1.22, respectively, where the negative sign means the velocity is in the opposite direction. These values should be compared to the THz yields given in Fig. 1(b), where the yields are consistent with the value of the average velocity. Even though we have not calculated the photocurrent, the average velocity which was calculated from the quantum model is an equivalent approximate quantity.

Note that the THz yield was calculated from time-frequency wavelet analysis, Eq. (5), i.e., $A_\omega(t_0, \omega)$. An example of $A_\omega(t_0, \omega)$ can be found in Fig. 6 of Ref. [9]. In Fig. 1(b), we plot the time-dependent growth of THz at 18 THz. On the
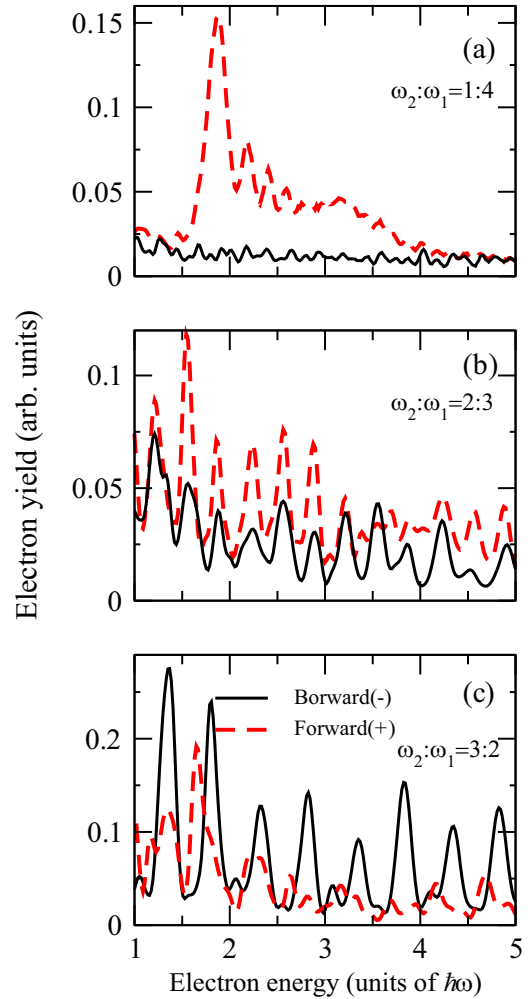
FIG. 2. Yields of ATI electrons calculated from Eq. (7) on the right side ($z > 0$, dashed red line) and on the left side ($z < 0$, solid black line) of the polarization axis generated by two-color laser pulses of various frequency ratios. (a) $\omega_2 : \omega_1 = 1 : 4$, (b) $2 : 3$, and (c) $3 : 2$. The laser parameters are the same as those in Fig. 1.

scale of Fig. 1(b), the growth of the THz signal with time is not clearly seen, but for the three curves ($\omega_2 : \omega_1 = 2 : 3$, $3:2$, and $1:4$) they grow from 271.2 to 277.2, from 207.5 to 212.2, and from 79.2 to 80.5, in arbitrary units, respectively. Their relative magnitudes are consistent with the DC terms calculated from the average velocity in Fig. 1(a) and are consistent with the expectation according to the PC model. Laser parameters used in the three calculations are given in the caption of Fig. 1.

B. Asymmetry in the ATI electron spectra

From the TDSE calculations, the ATI photoelectron distributions can be calculated. Figures 2(a)–2(c) show the asymmetric left-right electron energy distributions along the polarized axis for the three special frequency ratios. Such asymmetry is also reflected in the intensity of the photocurrent along each direction. We can obtain the asymmetry coefficient of the ATI spectra for the three cases by integrating the electrons in each direction for energies from zero to $2U_p$, where U_p is the

ponderomotive energy. For the three cases, the asymmetries are 0.06, 0.25, and −0.12, respectively. Their absolute values are consistent with the THz intensity shown in Fig. 1(b). Their signs are consistent with the direction of the electron velocity in Fig. 1(a), indicating that the DC electron current is biased toward the $+z$ direction for $\omega_2 : \omega_1 = 1 : 4$ and $2 : 3$ and the $-z$ direction for $\omega_2 : \omega_1 = 3 : 2$. This character of asymmetry is more clearly demonstrated by the energy distribution of photoelectrons obtained from quantum calculation, as shown in Figs. 2(a)– 2(c). In calculating the asymmetries, we used Eq. (8), where the probability of an electron signal on each side (+ or −) is integrated from threshold to $2U_p$. The values of the latter are 46.3, 8.7, and 3.9, in units of photon energy of the fundamental laser field, respectively.

The asymmetry of the photoelectron distribution also allows us to obtain more information on the THz waves, which will be further discussed below.

C. THz emission versus strong overlap of even- and odd-parity photoelectrons

We next address THz photon emission based on the ATI photoelectron spectra. To this end, we separate the compositions of odd- and even-parity photoelectrons by extracting contributions of odd- and even-integer orbital angular momentum quantum numbers of the continuum electron wave functions. The good overlap of even and odd photoelectron spectra guarantees a strong forward and backward asymmetry in the photoelectron spectra. Figures 3(a)–3(c) show the distributions of even- and odd-integer orbital angular momentum components versus electron energy. The region where the overlap is large in each frequency ratio is marked by a blue dotted ellipse. This overlap provides a measure of the probability amplitude for THz photon emission. Similar to a four-photon process in the combined two-color laser fields of the fundamental and its second harmonic [9], THz emission in two-color laser pulses of various frequency ratios can also be explained by multiphoton processes in the quantum picture.

Since each ATI peak has a narrow bandwidth [9,22], the even-odd peak overlap means that the electron can start from an intermediate state (generally, a high Rydberg state) by absorbing n_1 of ω_1 photons to a continuum state with energy $E + \epsilon$ with even angular quantum numbers or by absorbing n_2 of ω_2 photons to a continuum state with energy E with odd angular quantum numbers. Such pairs of states provide a dipole-allowed transition for THz photon emission with energy ϵ. Based on this picture, radiation of THz photons requires two conditions. First, because THz photon energy is low, the two continuum states involved in the transition require similar energies, i.e., $n_1\omega_1 \approx n_2\omega_2$, where n_1 and n_2 are irreducible integers. Second, if n_1 is an odd number, n_2 must be an even number and vice versa. In other words, the sum of n_1 and n_2 is an odd number. This is consistent with the conclusion reported by Kostin et al. [19].

In our model, besides providing the condition of the frequencies of the two-color laser, additional information on the yields of THz waves can be obtained from the energy distribution of photoelectrons obtained from the quantum calculations. When the above conditions are met, the values of n_1 and n_2 also will affect THz radiation intensity. When
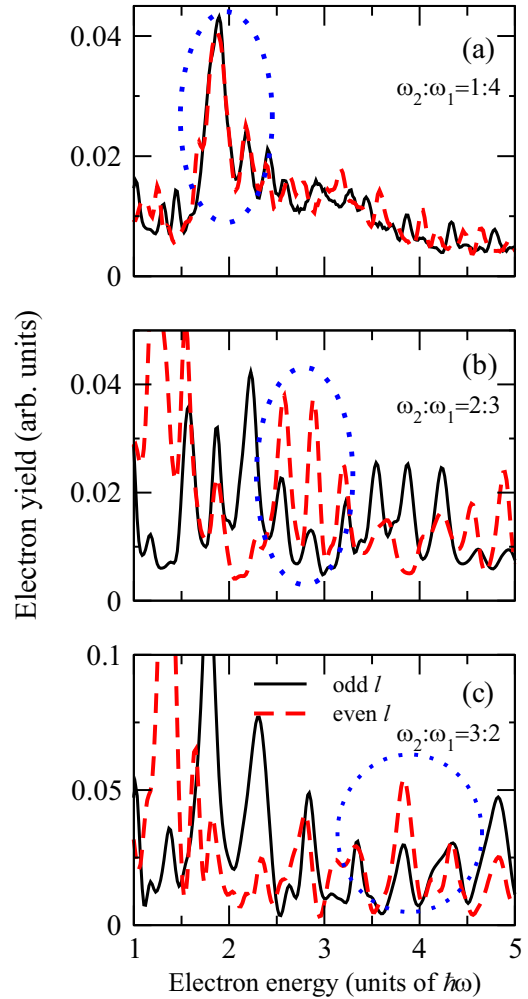
FIG. 3. The ATI spectra of electrons with odd- (solid black line) and even- (dashed red line) integer orbital angular momentum quantum numbers along the polarization direction for (a) $\omega_2 : \omega_1 = 1 : 4$, (b) $2 : 3$, and (c) $3 : 2$. The blue dotted ellipse indicates the region where odd- and even-parity photoelectrons coincide for each of the three cases. As the ratio of the frequency of the second laser with respect to the fixed frequency of the first laser increases from 1/4 to 2/3 to 3/2, the ellipse moves from low to higher energies.

their values are large, the electron needs to absorb many photons, leading to a smaller probability to attain continuum electrons and to weaker THz waves. For example, the lowest THz radiation intensity for the three cases in Fig. 1 occurs because the electron needs to absorb at least four photons from the second laser field (ω_2). Thus, THz radiation will be weak when n_1 or n_2 is large for a fixed laser intensity.

In addition, if the frequency ratios of the two laser fields are the same (for example, $\omega_2 : \omega_1 = 2 : 3$ and $3 : 2$ or $\omega_2 : \omega_1 = 1 : 2$ and $2 : 1$, etc.), the probabilities of absorbing multiple photons are the same based on the perturbation theory for the same laser strength. However, THz radiation will decrease as the frequency of the second laser increases with a fixed ω_1. For example, THz radiation is stronger when $\omega_2 = (2/3)\omega_1$ than when $\omega_2 = (3/2)\omega_1$, as shown in Fig. 1. Based on the multiphoton mixing model here, it is assumed that the

electrons start from the same Rydberg state. For the former case ($\omega_2 : \omega_1 = 2 : 3$), the electrons will absorb at least two fundamental photons or three ω_2 photons to achieve continuum states with similar energies and different parities. For the latter case ($\omega_2 : \omega_1 = 3 : 2$), the electrons will absorb at least three fundamental photons or two ω_2 photons to satisfy the THz radiation condition, and the electron will make a transition to a higher-energy continuum than the former case ($\omega_2 : \omega_1 = 2 : 3$). Thus, the THz radiation is weakened with a lower occupancy of continuum states. This condition can be seen from the results shown in Fig. 3. As the frequency of the second laser increases, the overlap between the even- and odd-parity photoelectron occurs at higher photoelectron energy (the blue dotted ellipse), and its occupation probability becomes smaller. We can also infer that THz radiation will be stronger when $\omega_2 : \omega_1 = 1 : 2$ compared to that when $\omega_2 : \omega_1 = 2 : 1$ when the laser intensities remains the same and so on.

D. Role of relative phase between the two-color fields and THz emission

Besides the selection of the appropriate combination of laser frequencies, the relative phase of the two laser fields also plays an important role in THz radiation. Taking the most widely discussed $(800 + 400)$-nm laser as an example, the relationship of THz amplitude to the phase difference of the two-color laser fields has been found to be quite controversial. According to the PC model, the THz amplitude is proportional to $\sin\varphi$. Thus, the THz emission is highest when $\varphi = \pi/2$. Another model is based on the third-order nonlinear four-wave mixing (FWM). In this model, the THz amplitude is proportional to $\cos\varphi$; thus, the optimal yield occurs at $\varphi = 0$ or π. Where or how do these two models work? In the third-order nonlinear FWM, clearly, it is for low laser intensity, and it does not involve continuum electrons directly. In the PC model, it is based on a classical description of continuum electrons where the emission step was not considered. One may want to argue that the PC model would work better in the tunnel ionization regime where typical THz emission experiments are carried out. Indeed, experiments in Refs. [29,33,34] appear to support the PC model, where optimal THz emissions were reported at $\varphi = \pi/2$. On the other hand, other experiments favored the prediction of the FWM model [3,5].

It is interesting to point out that the determination of the optimal phase for THz emission should be performed with a constant ionization yield since a change in the relative phase alone would alter the ionization yield. In addition, precise measurement of the absolute relative phase between two laser pulses in the laboratory is a great challenge. Thus, it is fair to say generally that the reported optimal phase difference for THz emission in a two-color field should be treated with caution. In Ref. [35], the authors mitigated these problems by measuring the THz emission and the generation of high-order harmonics together. Since the theory of high-order-harmonic generation (HHG) is much simpler than the theory for THz emission, the phase difference for maximal THz emission can be obtained from the HHG spectra, where the latter can be calculated accurately by solving the 3D TDSE. In

Ref. [35], the authors obtained the highest THz emission when $\varphi = 0.8\pi$ at the tunnel ionization laser intensity of $I_{800} = 2.3 \times 10^{14}$ W/cm^2, instead of $\varphi = \pi/2$ as predicted by the PC model. The difference from the PC model is 0.3π. If one were to use the FWM model, the optimum value would be $\varphi = \pi$, where the error would be 0.2π. In Ref. [11], from TDSE calculations, it was also found that the optimal relative phase for THz emission will vary with laser intensity. In combination with results from different calculations and experiments, it is fair to take the stand that the relative phase for optimal THz emission predicted by the PC model or the FWM model should be taken with caution. In our previous paper [22] we studied THz emission together with photoelectron spectra. Empirically, we found that for $(800 + 400)$-nm two-color fields, the relative phase for maximal THz emission is closer to the $\cos\varphi$ dependence, except by some additional phase shift. This dependence is similar to the prediction of the perturbative four-wave mixing model even though the generation of the THz field is a strong-field process. The underlying reason for this observation was left unexplained in Ref. [22].

In this article, we extend the four-photon mixing model to the multiphoton mixing case discussed above. We also discuss the phase dependence of the THz amplitude on the relative phase of the two-color laser fields for various frequency ratios. Take $\omega_2 : \omega_1 = 3 : 2$, for instance; we consider the final state u_{f_1} to be reached from some intermediate state u_i by absorbing three ω_1 photons, and a nearby state u_{f_2} can also be reached from the same intermediate state by absorbing two ω_2 photons. The amplitude for reaching each final state is viewed from the perturbation method,

$$a_{f_1 i}^{(3)} \propto E_{\omega_1}^3 \tag{11}$$

and

$$a_{f_2 i}^{(2)} \propto E_{\omega_2}^2 e^{-2i\varphi}, \tag{12}$$

respectively. For THz emission, the transition dipole from u_{f_1} to u_{f_2} is

$$
\begin{aligned}
d_x(t) &= \langle u_{f_2}|z|u_{f_1}\rangle + \langle u_{f_1}|z|u_{f_2}\rangle \\
&\propto \mathrm{Re}\big(a_{f_1 i}^{(3)*} a_{f_2 i}^{(2)}\big) \propto E_{\omega_1}^3 E_{\omega_2}^2 \cos 2\varphi.
\end{aligned} \tag{13}
$$

By associating THz emission with the dipole transition between continuum states u_{f_1} and u_{f_2}, we should get the same relationship of the THz amplitude to the laser parameters. However, due to the limitations of the perturbation model, the effect of complex atomic structure, and the shape of the laser pulse, this simple expression may deviate from quantum calculations.

We test the relative phase dependence of the THz amplitude for the case of $\omega_2 : \omega_1 = 3 : 2$ by solving TDSE, and the result is shown in Fig. 4(a). We observe that there are two full oscillations in the THz amplitudes within a 2π range of the relative phase, in agreement with Eq. (13). However, similar to the $\omega + 2\omega$ combined laser fields, the precise relative phase of the φ dependence differs from that predicted by the multiphoton model since effects like tunneling ionization and Coulomb potential were not accounted for [10,11].
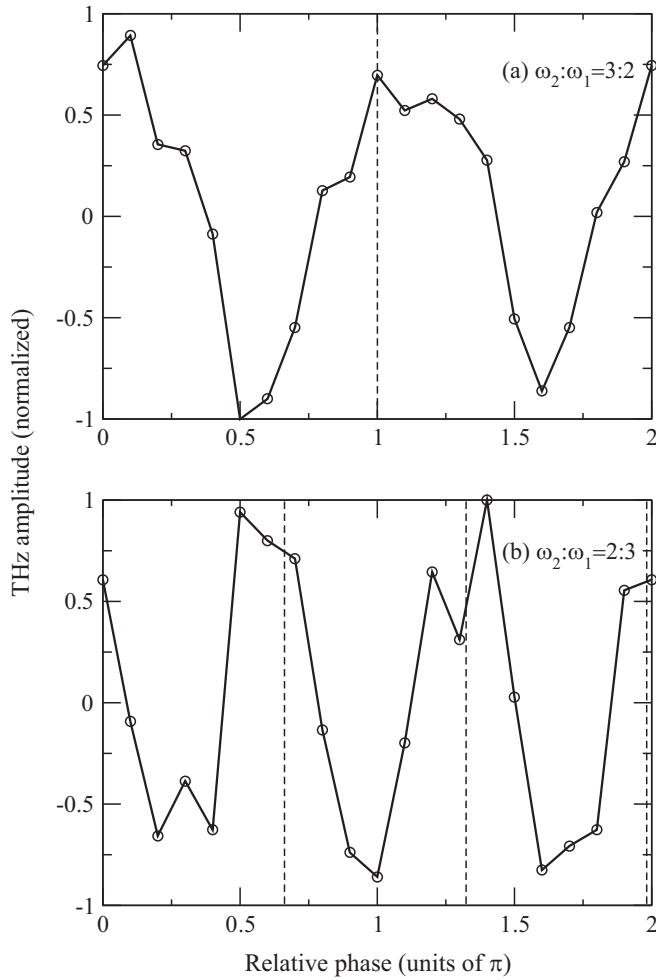
FIG. 4. The normalized THz emission versus the relative phase between the two colors of the driving laser. The amplitudes are obtained from the peak value of the wavelet transform [as in Fig. 1(b)], and their signs are from the asymmetry of the ATI spectrum on the $\pm z$ sides [see Eq. (8)]. (a) $\omega_2 : \omega_1 = 3 : 2$ and (b) $\omega_2 : \omega_1 = 2 : 3$. The dashed lines indicate a complete oscillation of the THz amplitude with the change in the relative phase. The laser parameters are the same as those in Fig. 1 except that the laser duration is extended to 60 oc of ω_1 in (b).

Extending this multiphoton model to two-color fields of other frequency ratios, we get the universal formula

$$E_{\mathrm{THz}} \propto \cos(n_2 \varphi), \qquad (14)$$

where n_2 is the minimum number of ω_2 photons needed to reach the THz radiation conditions stated above, for example, $n_2 = 2$ when $\omega_2 : \omega_1 = 3 : 2$ and $n_2 = 3$ when $\omega_2 : \omega_1 = 2 : 3$. For the latter case, the frequency ω_2 of the second laser is decreasing; for the same 20 oc of ω_1, the number of cycles for ω_2 is decreased, but more laser photons are needed. We found that clear phase dependence cannot be observed for $\omega_2 : \omega_1 = 2 : 3$ under the same 20 oc of ω_1. We extend the duration of the laser fields to 60 oc of ω_1; the calculated results are then closer to the above theoretical prediction. The clear dependence of THz radiation on the relative phase φ can be observed, as shown in Fig. 4(b). Three full oscillations

appear in the THz amplitudes within a 2π range of the relative phase. We have marked a complete cycle with two dashed lines in Fig. 4(b), located at $\varphi = 0.67\pi$ and $\varphi = 1.33\pi$; that is, its amplitude is proportional to $\cos(3\pi)$, as predicted in Eq. (14). Similar to the case of $\omega + 2\omega$ laser fields, THz wave dependence on the relative phase φ of the two-color laser fields will deviate from the simple cosine relationship exactly. And the optimal phase of the THz wave will also change with different laser parameters and ionization rates. On the other hand, the prediction of Eq. (14) appears to be quite accurate, except that one can expect a constant phase shift that will change with laser intensity and target.

IV. THz GENERATION IN MULTICOLOR LASER PULSES

It was proposed [21] that THz conversion can be greatly improved with well-designed multicolor pulses of the form

$$E(t) = \sum_{k=1}^{N} E_k(t) = \sum_{k=1}^{N} f_k(t) a_k \cos(k\omega_0 t + \varphi_k). \qquad (15)$$

Reference [21] showed that a multicolor sawtooth wave-form laser pulse can be obtained by setting $a_k = 1/k$ and $\varphi_k = (-1)^k \pi/2$. For such a pulse, according to the PC model, the largest drift velocity can be acquired, and the THz wave can be efficiently enhanced. Similar to the case of $\omega_2 : \omega_1 = 2 : 1$ pulses, in discussing the optimum phase for THz radiation, the predictions by the semiclassical photocurrent model are expected to differ from those obtained by solving the 3D TDSE [10,11]. From the quantum calculation and the multiphoton mixing model, such studies would provide a complementary perspective to the mechanism of THz generation by multicolor pulses.

We analyze the enhancement of THz wave generation for such a three-color pulse in the form of Eq. (15), which has a sine-square form envelope $f(t)$ and the same 20 oc of the laser pulse of frequency ω_0. From the multiphoton ionization model, the combination of multiple frequencies would provide more possibilities for the multiple ionization pathways required for THz emissions. Electrons can absorb laser photons of different energies to reach the nearly degenerate final states, u_{f_1} and u_{f_2}, as discussed in Sec. III D. For $N = 3$, for example, several ionization paths favorable to THz radiation will exist for a laser combination of $\omega_3 : \omega_2 : \omega_1 = 3 : 2 : 1$, where $\omega_{1,2,3}$ is the frequency of the three-color incident laser fields. Using the sawtooth wave form given in Eq. (15) and phases of $\varphi_{1,2,3} = -\pi/2, \pi/2, -\pi/2$, we calculated the degree of overlap between the even-odd angular momentum mixture within each ATI peak, as shown in Fig. 5(a). The large overlap shown guarantees that THz photon emission is large according to the present model.

Frequency mixing has been emphasized in the multiphoton mixing model for THz enhancement. However, THz radiation can be even stronger if the relative phases φ_k of the incident laser fields of Eq. (15) are adjusted. Claiming optimal relative phases among the three color fields for the highest THz emission with fixed total ionization rates would be difficult to do in true TDSE calculations or in experiments. However, to test the correlation between THz emission and the asymmetry of photoelectron spectra for the three-color fields, we have found
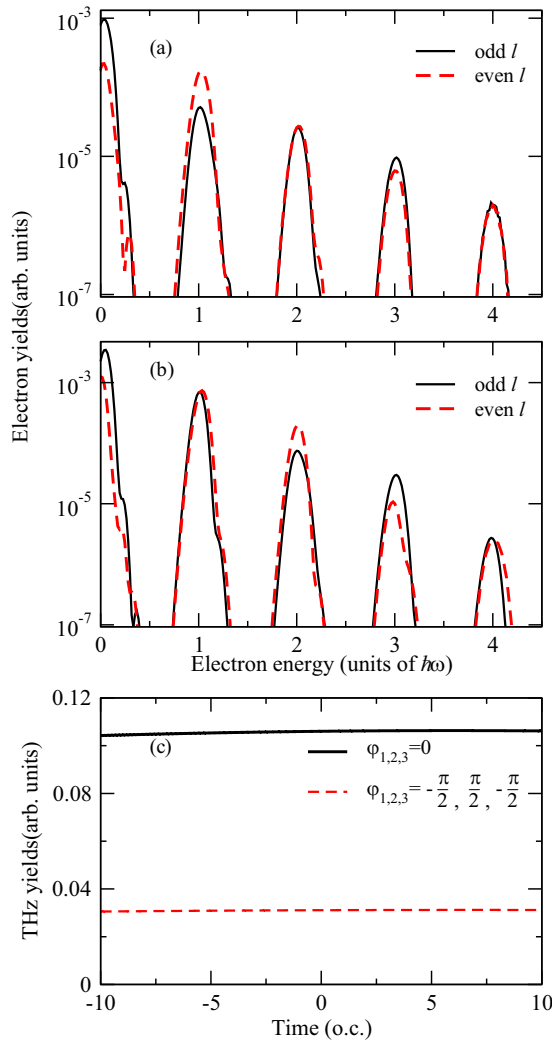
FIG. 5. The ATI spectra of an electron with even- (solid black line) and odd- (dashed red line) integer orbital quantum numbers along the polarization direction for the laser pulse of Eq. (15) when (a) $\varphi_{1,2,3} = -\pi/2, \pi/2, -\pi/2$ (sawtooth shaped) and (b) $\varphi_{1,2,3} = 0, 0, 0$ for the $N = 3$ cases. The corresponding time profiles of the 18-THz wave for the two cases are shown in (c). The fundamental laser pulse is set to be 800 nm, and intensity is 5×10^{12} W/cm^2.

that if the relative phases are all set to zero, we obtain even stronger THz signals by analyzing the degree of overlap of even- and odd-parity photoelectrons in the ATI spectra. This conclusion is explained in Fig. 5. Figures 5(a) and 5(b) display the even- and odd-parity photoelectron overlap for the three phases of $\varphi_{1,2,3} = -\pi/2, \pi/2, -\pi/2$ and $\varphi_{1,2,3} = 0, 0, 0$, respectively. Clearly, the overlap is stronger in Fig. 5(b) than in Fig. 5(a). According to the present model, the one with phases $\varphi_{1,2,3} = 0, 0, 0$ would be stronger. The THz signals shown in Fig. 5(c) obtained from our 3D TDSE calculations are in agreement with the prediction.

It should be pointed out that the conclusion presented in Fig. 5 was based on THz generated with low fields. The results should not be taken as a prediction for other cases. However,

the link of higher THz generation with the degree of overlap between even- and odd-parity photoelectron distributions is valid. The latter criterion still requires accurate theoretical calculations of the ATI spectra without providing any guidance for experimentalists.

V. CONCLUSIONS

In this article, we studied the correlation of THz generation with the nature of the asymmetry of photoelectron spectrum along the polarization axis by two- and three-color laser pulses with various frequency ratios. THz photons are generated through free-free transitions between continuum states of similar energies but of different parities. A multiphoton mixing model was further used to identify conditions for efficient THz generation. The models were used to interpret the relation between THz emission and the photoelectron spectra obtained simultaneously from solving the TDSE for various frequency combinations of the two-color and three-color pulses. Through the numerical results, we first confirm that THz radiation strength can be related to the degree of overlap between the even-parity-dominated electrons and the odd-parity-dominated electrons within each ATI peak. The importance of such a large overlap helps us to confirm the relevance of the multiphoton mixing conditions in THz emissions.

For two-color laser fields with different frequency ratios, the frequency relationship that favors THz radiation is $n_1\omega_1 \approx n_2\omega_2$, and the sum of n_1 and n_2 is an odd natural number. Here n_1 and n_2 are the minimum numbers of photons needed to be absorbed to reach two continuum states of nearly identical energies. Once the condition is satisfied, it guarantees that the two neighboring states have opposite parities to favor free-free transitions with the emission of THz photons. For large n_1 and n_2 that satisfy the above condition, THz emission is weak because multiphoton ionization of the continuum states from an intermediate Rydberg state decreases with the number of photons absorbed. With this multiphoton mixing model, the results from the TDSE calculations, such as the role of the frequency combination, can be nicely interpreted.

For three-color lasers, predictions of the PC model have shown that THz radiations can be enhanced with certain frequency combinations together with certain relative phase combinations. Our TDSE calculations do not support the prediction of the PC model. On the other hand, our conclusion that a large overlap of even-party and odd-parity photoelectron spectra would lead to stronger THz generation was also confirmed to apply to three-color driving lasers.

[1] *Sensing with Terahertz Radiation*, edited by D. Mittleman (Springer, Berlin, 2002).

[2] J. F. Federici, B. Schulkin, F. Huang, D. Gary, R. Barat, F. Oliveira, and D. Zimdars, Semicond. Sci. Technol. **20**, S266 (2005).

[3] X. Xie, J. Dai, and X.-C. Zhang, Phys. Rev. Lett. **96**, 075005 (2006).

[4] J. Dai, X. Xie, and X.-C. Zhang, Phys. Rev. Lett. **97**, 103903 (2006).

[5] D. J. Cook and R. M. Hochstrasser, Opt. Lett. **25**, 1210 (2000).

[6] V. A. Andreeva, O. G. Kosareva, N. A. Panov, D. E. Shipilo, P. M. Solyankin, M. N. Esaulkov, P. González de Alaiza Martínez, A. P. Shkurinov, V. A. Makarov, L. Bergé, and S. L. Chin, Phys. Rev. Lett. **116**, 063902 (2016).

[7] A. A. Silaev and N. V. Vvedenskii, Phys. Rev. Lett. **102**, 115005 (2009).

[8] N. Karpowicz and X.-C. Zhang, Phys. Rev. Lett. **102**, 093001 (2009).

[9] Z. Zhou, D. Zhang, Z. Zhao, and J. Yuan, Phys. Rev. A **79**, 063413 (2009).

[10] A. A. Silaev, M. Y. Ryabikin, and N. V. Vvedenskii, Phys. Rev. A **82**, 033416 (2010).

[11] W. Chen, Y. Huang, C. Meng, J. Liu, Z. Zhou, D. Zhang, J. Yuan, and Z. Zhao, Phys. Rev. A **92**, 033410 (2015).

[12] M. D. Thomson, V. Blank, and H. G. Roskos, Opt. Express **18**, 023173 (2010).

[13] J. Dai, N. Karpowicz, and X.-C. Zhang, Phys. Rev. Lett. **103**, 023001 (2009).

[14] M. Kress, T. Löffer, S. Eden, M. Thomson, and H. G. Roskos, Opt. Lett. **29**, 1120 (2004).

[15] Y. S. You, T. I. Oh, and K. Y. Kim, Phys. Rev. Lett. **109**, 183902 (2012).

[16] T. Löffler, M. Kress, M. Thomson, and H. G. Roskos, Acta. Phys. Pol. A **107**, 99 (2005).

[17] W.-M. Wang, Y.-T. Li, Z.-M. Sheng, X. Lu, and J. Zhang, Phys. Rev. E **87**, 033108 (2013).

[18] W.-M. Wang, Z.-M. Sheng, Y.-T. Li, Y. Zhang, and J. Zhang, Phys. Rev. A **96**, 023844 (2017).

[19] V. A. Kostin, I. D. Laryushin, A. A. Silaev, and N. V. Vvedenskii, Phys. Rev. Lett. **117**, 035003 (2016).

[20] L.-L. Zhang, W.-M. Wang, T. Wu, R. Zhang, S.-J. Zhang, C.-L. Zhang, Y. Zhang, Z.-M. Sheng, and X.-C. Zhang, Phys. Rev. Lett. **119**, 235001 (2017).

[21] P. González de Alaiza Martínez, I. Babushkin, L. Bergé, S. Skupin, E. Cabrera-Granado, C. Köhler, U. Morgner, A. Husakou, and J. Herrmann, Phys. Rev. Lett. **114**, 183901 (2015)

[22] Z. Zhou, X. Wang, and C. D. Lin, Phys. Rev. A **95**, 033418 (2017).

[23] D. O. Harris, G. G. Engerholm, and W. D. Gwinn, J. Chem. Phys. **43**, 1515 (1965).

[24] A. S. Dickinson and P. R. Certain, J. Chem. Phys. **49**, 4209 (1968).

[25] J. C. Light and R. B. Walker, J. Chem. Phys. **65**, 4272 (1976).

[26] X. M. Tong and S.-I. Chu, Chem. Phys. **217**, 119 (1997).

[27] M. Thomson, M. Kreß, T. Löffer, and H. G. Roskos, Laser Photonics Rev. **1**, 349 (2007).

[28] T. Bartel, P. Gaal, K. Reimann, M. Woerner, and T. Elsaesser, Opt. Lett. **30**, 2805 (2005).

[29] I. Babushkin, S. Skupin, A. Husakou, C. Köhler, E. Cabrera-Granado, L. Bergé, and J. Herrmann, New J. Phys. **13**, 123029 (2011).

[30] A. Nguyen, K. J. Kaltenecker, J. C. Delagnes, B. Zhou, E. Cormier, N. Fedorov, R. Bouillaud, D. Descamps, I. Thiele, S. Skupin, P. U. Jepsen, and L. Bergé, Opt. Lett. **44**, 1488 (2019).

[31] S. Chelkowski, A. D. Bandrauk, and A. Apolonski, Phys. Rev. A **70**, 013815 (2004).

[32] X. Zheng, M.-M. Liu, H. Xie, P. Ge, M. Li, and Y. Liu, Phys. Rev. A **92**, 053422 (2015).

[33] K. Y. Kim, J. H. Glownia, A. J. Taylor, and G. Rodriguez, Opt. Express **15**, 4577 (2007).

[34] M. Li, W. Lia, Y. Shi, P. Lu, H. Pan, and H. Zeng, Appl. Phys. Lett. **101**, 161104 (2012).

[35] D. Zhang, Z. Lu, C. Meng, X. Du, Z. Zhou, Z. Zhao, and J. Yuan, Phys. Rev. Lett. **109**, 243002 (2012).